Computer Assisted Mechanics and Engineering Sciences, 4: 383–396, 1997.

A Trefftz simplified method for the computation of elastic structures

C. Hochard, P. Ladevèze and L. Proslier
Laboratoire de Mécanique et Technologie, ENS de Cachan, CNRS, Université Paris VI, 61 avenue du président Wilson, 94235 Cachan, France

(Received December 20, 1996)

This paper presents a method for a quick evaluation of stresses and displacements for elastostatic problems. A set of polynomial Trefftz functions and a variational formulation are introduced for solving elastostatic problems for simple star-shaped domains. It is shown, through examples, that this approximation allows the computation of the interior large wavelength effects. By a procedure for coupling separate domains, this method is extended to more complex structures, which is a natural extension of the above variational formulation. A discretization of the structure into large substructures, an easy to use and quick computation of the interior solution justify that this method can be termed "simplified". Comparisons with other similar methods are also shown.

1. Introduction

Up until now, structural analysis has used the Finite Element Method (FEM) [18], or the Boundary Element Method (BEM) [2]. These approaches can solve most problems, but they can be time consuming in analyzing very complex structures. There are many situations, such as optimization processes of machine pieces, where a less precise but faster analysis is sufficient. Between FEM and elementary analytical techniques, such as Strength of Materials, methods exist, which can be termed "simplified" in that they make it possible for stresses and displacements to be evaluated quickly and accurately. These methods, less precise than FEM or BEM, make use of some knowledge of the exact solution to the problem.

As one of these methods, the simplified approach presented herein is a Trefftz method that allows the computation of large wavelength effects: in elastostatic problems, stresses vary only slightly inside a massive body. The short wavelength effects, which appear only around the edges, can be calculated in a subsequent step. However, very often in the preliminary planning of engineering works, the computation of edge effects is either not necessary (optimization of the structure stiffness, for example) or not possible (the geometry of the structure is not precisely defined)

The class of Trefftz methods is based on the existence of complete systems of non-singular displacement solutions which fulfill a priori the governing differential equation of the problem [5–7]. There are several alternative variational formulations of a given problem [10,11].

In our approach, the approximation is built from the mathematical structure of the solutions. This approximation, using Trefftz functions, is representative of the interior effect. A variational formulation for a simple domain, which is consistent with this approximation and differs from the classical ones used in Trefftz methods [16,17], is then introduced. It should be noted that this formulation can be used for ill posed problems, where prescribed displacements and forces are given on the same boundary. The extension to more complex structures is possible by using a direct coupling substructuring technique.

2. TREFFTZ APPROXIMATION

The objective herein is the construction of a set of interpolation functions representative of the interior effect. The following results are obtained from the study of the mathematical structure of the solutions for star-shaped domains.

The elasticity problem, where body forces are equal to zero, is written as follows:

To find $\mathbf{u}$ *displacement field, such that:*

$$\begin{aligned} &\operatorname{div}\boldsymbol{\sigma}(\mathbf{u}) = 0 \quad &&\text{in} \quad \Omega\,, \\ &\mathbf{u} = \mathbf{u}_d \quad &&\text{on} \quad \partial_1\Omega\,, \\ &\boldsymbol{\sigma}(\mathbf{u})\mathbf{n} = \mathbf{f}_d \quad &&\text{on} \quad \partial_2\Omega\,, \\ &\boldsymbol{\sigma}(\mathbf{u}) = \mathbf{K}\boldsymbol{\varepsilon}(\mathbf{u})\,, \end{aligned} \tag{1}$$

where displacements $\mathbf{u}_d$ and forces $\mathbf{f}_d$ are prescribed on $\partial_1\Omega$ and $\partial_2\Omega$, respectively. $\mathbf{K}$ and $\boldsymbol{\varepsilon}(\mathbf{u})$ are the elastic tensor and the strain tensor. This problem has a unique solution when $\mathbf{u}_d$ and $\mathbf{f}_d$ satisfy the classical regularity conditions [4]. By using suitable coordinates and variables, the elasticity problem for a star-shaped domain is replaced by a fictitious straight semi-infinite elastic beam problem [9,12], to which results deduced from Saint-Venant's principle are applied [13,14]. For star-shaped domains, the study of the mathematical structure of the solution favors a representation of the solution using polynomials with respect to the x, y and z coordinates and fulfilling the internal equilibrium equations.

We note: $U_e = \{\mathbf{u} \text{ finite energy displacements, } \operatorname{div}\mathbf{K}\boldsymbol{\varepsilon}(\mathbf{u}) = 0\}\,.$

It can be shown that, for inner points of the domain, a good approximation of the displacement solution u is obtained with polynomials belonging to the following finite-dimensioned subspace:

$$U_e^p = \{\mathbf{u} \text{ polynomial of degree } \leq p \,|_{x,y,z}, \operatorname{div}\mathbf{K}\boldsymbol{\varepsilon}(\mathbf{u}) = 0\}\,. \tag{2}$$

These Trefftz functions are representative of the interior effect. Similar results have been obtained for plates in the framework of the Kirchhoff–Love theory [8].

3. VARIATIONAL FORMULATION FOR A SIMPLE DOMAIN

3.1. Problem formulation

A variational formulation is introduced, which is consistent with the above approximation. This formulation will take the boundary conditions into account. The problem (1) is replaced by an equivalent formulation [12] which can be written as:

To find $\mathbf{u}$ *belonging to* U_e *such that:*

$$\forall \mathbf{u}^* \in U_e \quad \int_{\partial_1\Omega} \boldsymbol{\sigma}(\mathbf{u}^*)\mathbf{n}\cdot(\mathbf{u}-\mathbf{u}_d)\,\mathrm{d}\Gamma + \int_{\partial_2\Omega} \mathbf{u}^*\cdot(\boldsymbol{\sigma}\mathbf{n}-\mathbf{f}_d)\,\mathrm{d}\Gamma = 0\,, \tag{3}$$

where $\mathbf{n}$ is the outward unit vector normal to $\partial\Omega$, $\boldsymbol{\sigma}(\mathbf{u}) = \mathbf{K}\boldsymbol{\varepsilon}(\mathbf{u})$.

Let $\mathbf{u}_v$ be the solution to (1), $\boldsymbol{\varepsilon}_v = \boldsymbol{\varepsilon}(\mathbf{u}_v)$, $\boldsymbol{\sigma}_v = \mathbf{K}\boldsymbol{\varepsilon}(\mathbf{u}_v)$. It is clear that $\mathbf{u}_v$ is a solution to (3). Thus, to demonstrate the equivalence with (1), it suffices to show the uniqueness of the solution. To this end, two solutions $\mathbf{u}_1$ and $\mathbf{u}_2$ are considered. The difference $\mathbf{u} = \mathbf{u}_1 - \mathbf{u}_2$ belongs to U_e and solves the following problem deduced from (3), with $\mathbf{u}_d = 0$ and $\mathbf{f}_d = 0$:

$$\forall \mathbf{u}^* \in U_e \quad \int_{\partial_1\Omega} \boldsymbol{\sigma}(\mathbf{u}^*)\mathbf{n}\cdot\mathbf{u}\,\mathrm{d}\Gamma + \int_{\partial_2\Omega} \mathbf{u}^*\cdot\boldsymbol{\sigma}(\mathbf{u})\mathbf{n}\,\mathrm{d}\Gamma = 0\,. \tag{4}$$

For $\mathbf{u}^* = \mathbf{u}$ and by using Stokes' formula, (4) gives:

$$\int_\Omega \mathrm{Tr}\,[\boldsymbol{\varepsilon}(\mathbf{u})\mathbf{K}\boldsymbol{\varepsilon}(\mathbf{u})]\,\mathrm{d}\Omega = 0 \quad \Leftrightarrow \quad \boldsymbol{\varepsilon}(\mathbf{u}) = 0.$$

If $\boldsymbol{\varepsilon}(\mathbf{u})$ is zero, $\mathbf{u}$ is a rigid body displacement $\mathbf{u} = \mathbf{u}(o) + \mathbf{w} \wedge \mathbf{OM}$. Relation (4) is then written as follows:

$$\forall \mathbf{u}^* \in U_e, \quad \mathbf{u}(o) \cdot \int_{\partial_1\Omega} \boldsymbol{\sigma}(\mathbf{u}^*)\mathbf{n}\,\mathrm{d}\Gamma + \mathbf{w} \cdot \int_{\partial_1\Omega} \mathbf{OM} \wedge \boldsymbol{\sigma}(\mathbf{u}^*)\mathbf{n}\,\mathrm{d}\Gamma = 0.$$

If the area of $\partial_1\Omega$ is different from zero or different from the area of $\partial\Omega$, this relation gives $\mathbf{u}(o) = \mathbf{0}$ and $\mathbf{w} = \mathbf{0}$, thus the solution is unique. In finite dimension, the approximation consists of replacing U_e by the subset U_e^p. As with problem (3), the uniqueness of stresses is obtained. In order to demonstrate the uniqueness of displacements, it is necessary that the above relation (with U_e^p) yield $\mathbf{u}(o) = \mathbf{0}$ and $\mathbf{w} = \mathbf{0}$. This is the case if the number of equations is sufficient. This step influences the choice of U_e^p and depends on the type of structures being studied.

Remarks:

- This formulation is not derived from a minimisation or saddle-point problem because it is not symmetric: when Stokes' formula is used, problem (3), with U_e^p, can be written as:

  To find $\mathbf{u}$ *belonging to* U_e^p *such that:* $\forall \mathbf{u}^* \in U_e^p$,

$$\begin{aligned} &\int_\Omega \mathrm{Tr}\,[\boldsymbol{\varepsilon}(\mathbf{u})\mathbf{K}\boldsymbol{\varepsilon}(\mathbf{u}^*)]\,\mathrm{d}\Omega + \int_{\partial\Omega} (\boldsymbol{\sigma}(\mathbf{u}^*)\mathbf{n} \cdot \mathbf{u} - \mathbf{u}^* \cdot \boldsymbol{\sigma}(\mathbf{u})\mathbf{n})\,\mathrm{d}\Gamma \\ &\qquad = \int_{\partial_2\Omega} \mathbf{f}_d \cdot \mathbf{u}^*\,\mathrm{d}\Gamma + \int_{\partial_1\Omega} \mathbf{u}_d \cdot \boldsymbol{\sigma}(\mathbf{u}^*)\mathbf{n}\,\mathrm{d}\Gamma\,. \end{aligned} \tag{5}$$

- The strain energy can be written in the following simple form (with $\mathbf{u}^* = \frac{1}{2}\mathbf{u}$):

$$\frac{1}{2}\int_\Omega \mathrm{Tr}\,[\boldsymbol{\varepsilon}(\mathbf{u}_v)\mathbf{K}\boldsymbol{\varepsilon}(\mathbf{u}_v)]\,\mathrm{d}\Omega = \frac{1}{2}\int_{\partial_1\Omega} \boldsymbol{\sigma}(\mathbf{u}_v)\mathbf{n} \cdot \mathbf{u}_d\,\mathrm{d}\Gamma + \frac{1}{2}\int_{\partial_2\Omega} \mathbf{u}_v \cdot \mathbf{f}_d\,\mathrm{d}\Gamma\,. \tag{6}$$

- It is possible to extend the formulation in (3) to other linear boundary conditions. For example, mixed-boundary conditions on $\partial\Omega = \partial_1\Omega \cup \partial_2\Omega \cup \partial_3\Omega$ can be considered: prescribed displacement on $\partial_1\Omega$, prescribed load on $\partial_2\Omega$ and bilateral contact without friction on $\partial_3\Omega$. The boundary conditions on $\partial_3\Omega$ are:

  $\mathbf{u} \cdot \mathbf{n} = \mathbf{v}_d$

  $\Pi\boldsymbol{\sigma}(\mathbf{u}) \cdot \mathbf{n} = \mathbf{T}_d$ where Π is the projection's operator on the tangent plane to $\partial_3\Omega$.

  The extension of (3) for these boundary conditions is:

  To find $\mathbf{u}$ *belonging to* U_e *such that* $\forall \mathbf{u}^* \in U_e$,

$$\begin{aligned} &\int_{\partial_1\Omega} \boldsymbol{\sigma}(\mathbf{u}^*) \cdot \mathbf{n} \cdot (\mathbf{u} - \mathbf{u}_d)\,\mathrm{d}\Gamma + \int_{\partial_2\Omega} \mathbf{u}^* \cdot (\boldsymbol{\sigma}(\mathbf{u}^*)\mathbf{n} - \mathbf{f}_d)\,\mathrm{d}\Gamma \\ &\quad + \int_{\partial_3\Omega} [\boldsymbol{\sigma}(\mathbf{u}^*)\mathbf{n} \cdot (\mathbf{u} \cdot \mathbf{n} - \mathbf{u}_d) + \mathbf{u}^* \cdot (\Pi\boldsymbol{\sigma}(\mathbf{u})\mathbf{n} - \mathbf{T}_d)]\,\mathrm{d}\Gamma = 0\,. \end{aligned} \tag{7}$$

As with problem (3), equivalence with the reference problem has been obtained.

This formulation can be used for ill posed problems, where prescribed displacements and forces are given on the same boundary. Let displacement $\mathbf{u}$ and force $\boldsymbol{\sigma}(\mathbf{u})\mathbf{n}$ both be prescribed on the

some boundary $\partial_3\Omega$: $\mathbf{u} = \mathbf{V}'_d$ and $\boldsymbol{\sigma}(\mathbf{u})\mathbf{n} = \mathbf{T}'_d$. For these boundary conditions, the problem can be written as:

To find $\mathbf{u}$ *belonging to* U_e *such that* $\forall \mathbf{u}^* \in U_e$,

$$\int_{\partial_1\Omega} \boldsymbol{\sigma}(\mathbf{u}^*)\mathbf{n}\cdot(\mathbf{u}-\mathbf{u}_d)\,\mathrm{d}\Gamma + \int_{\partial_2\Omega} \mathbf{u}^*\cdot(\boldsymbol{\sigma}(\mathbf{u}^*)\mathbf{n}-\mathbf{f}_d)\,\mathrm{d}\Gamma + \frac{1}{2}\int_{\partial_3\Omega} \left[\boldsymbol{\sigma}(\mathbf{u}^*)\mathbf{n}\cdot(\mathbf{u}-\mathbf{V}'_d) + \mathbf{u}^*\cdot(\boldsymbol{\sigma}(\mathbf{u})\mathbf{n}-\mathbf{T}'_d)\right]\mathrm{d}\Gamma = 0\,. \tag{8}$$

Problem (8) has, at most, one solution provided one exists for adequate boundary conditions.

3.2. Numerical implementation

For plane stress, we use the polynomial function with sets of degree lower than or equal to 3 which fulfill the governing differential equations (ν denotes Poisson's ratio):

$$\mathbf{u} = \sum_{i=1}^{14} a_i \mathbf{u}^i\,, \qquad a_i \in \mathbf{R}$$

with $\mathbf{u}^i \in U_e^3 = \{\mathbf{u} \text{ polynomial of degree } \leq 3,\ \mathrm{div}\,\mathbf{K}\boldsymbol{\varepsilon}(\mathbf{u}) = 0\}$, $\dim U_e^3 = 14$.

The set of vectors of degree n', $n \geq 1$, representing the equilibrium equations is of dimension 4. The set of polynomial functions is:

$$U_e^3 : \left[\begin{Bmatrix}0\\1\end{Bmatrix}, \begin{Bmatrix}1\\0\end{Bmatrix}, \begin{Bmatrix}y\\-x\end{Bmatrix}, \begin{Bmatrix}y\\x\end{Bmatrix}, \begin{Bmatrix}x\\0\end{Bmatrix}, \begin{Bmatrix}0\\y\end{Bmatrix}, \begin{Bmatrix}x^2-y^2\\-2xy\end{Bmatrix}, \begin{Bmatrix}-\nu x^2\\2xy\end{Bmatrix}, \begin{Bmatrix}2xy\\-\nu y^2-x^2\end{Bmatrix}, \begin{Bmatrix}-2xy\\y^2-x^2\end{Bmatrix}, \begin{Bmatrix}x^3-3xy^2\\y^3-3x^2y\end{Bmatrix}, \begin{Bmatrix}y^3-3x^2y\\-x^3+3xy^2\end{Bmatrix}, \begin{Bmatrix}\nu x^3+3xy^2\\-\nu y^3-3x^2y\end{Bmatrix}, \begin{Bmatrix}(3+\nu)y^3-3(1-\nu)x^2y\\(3+\nu)x^3-3(1-\nu)xy^2\end{Bmatrix}\right]. \tag{9}$$

The variational formulation (5) leads to a system of algebraic equations for the unknown coefficients a_i:

$$\mathbf{K}\mathbf{a} = \mathbf{s}$$

where

$$\begin{aligned} K^{kl} &= \int_\Sigma \mathrm{Tr}\left[\boldsymbol{\varepsilon}\left(\mathbf{u}^k\right)\mathbf{K}\boldsymbol{\varepsilon}\left(\mathbf{u}^l\right)\right]\mathrm{d}\Omega + \int_{\partial_1\Sigma}\left(\boldsymbol{\sigma}(\mathbf{u}^k)\mathbf{n}\cdot\mathbf{u}^l - \mathbf{u}^k\cdot\boldsymbol{\sigma}(\mathbf{u}^l)\mathbf{n}\right)\mathrm{d}\Gamma\,, \\ s^l &= \int_{\partial_2\Sigma}\mathbf{f}_d\cdot\mathbf{u}^l\,\mathrm{d}\Gamma + \int_{\partial_1\Sigma}\mathbf{u}_d\cdot\boldsymbol{\sigma}(\mathbf{u}^l)\mathbf{n}\,\mathrm{d}\Gamma\,. \end{aligned} \tag{10}$$

The symbolic mathematical software Macsyma [15] has been used to derive the expressions of the various matrices associated with the polynomial interpolation functions and with the variational formulation. For example:

$$\boldsymbol{\sigma}(\mathbf{u}^{10})\mathbf{n}\cdot\mathbf{u}^{11} - \mathbf{u}^{10}\cdot\boldsymbol{\sigma}(\mathbf{u}^{11})\mathbf{n} = (\nu-1)\left(n_y y^4 - 4n_x xy^3 + 5n_y x^4 - 4n_x x^3 y + 6n_y x^2 y^2\right)$$

and integrals of the polynomials y^4, $xy^3, \ldots$ over the boundary $\partial_1\Omega = [A, B]$ are written in terms of (A, B) coordinates.

4. Study of the solutions for a simple domain

4.1. Comparison with a finite element result

A square plate is chosen as numerical example. The boundary is clamped at $y = 0$, and the displacement $\mathbf{u} \cdot x$ on Γ is prescribed (Fig. 1), $\mathbf{u} \cdot y = 0$ on Γ. The reference solution is obtained from a finite element analysis, and von Mises's equivalent stresses σ^* are plotted:

$$\sigma^* = \left(\sigma_{xx}^2 + \sigma_{yy}^2 - \sigma_{xx}\sigma_{yy} + 3\sigma_{xy}^2\right)^{1/2},$$

Let σ_{fe}^* be the finite element solution (4-node quadrilateral elements, 1600 elements, Fig. 2) and σ_{sm}^* be the equivalent stress obtained from our simplified method (Fig. 3). A comparison between these results is given (Fig. 4) by plotting $\bar{\sigma}_1^*$, with $\bar{\sigma}_1^* = \left|\sigma_{\text{sm}}^* - \sigma_{\text{fe}}^*\right| / \sigma_{\text{ave}}^*$ where σ_{ave}^* corresponds to the average value of the finite element equivalent stress. For this example, $\sigma_{\text{ave}}^* = 1000$ Mpa. The lightest zone corresponds to an error of less than 20 per cent; a high level of agreement is obtained inside the plate, but the stress concentrations along the outer edge have been underestimated.

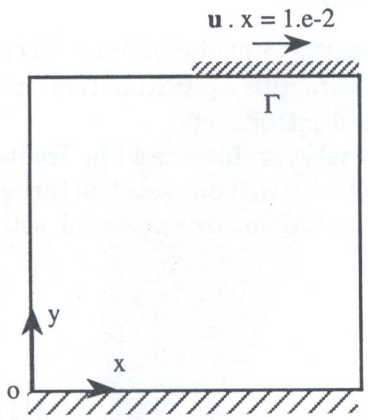

Fig. 1. Plate with prescribed displacements

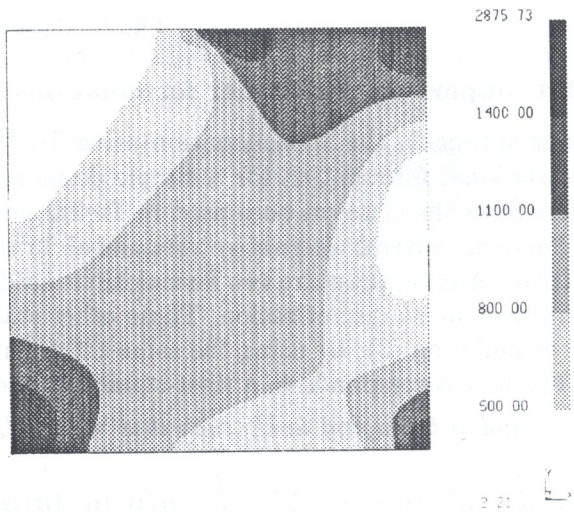

Fig. 2. Equivalent stress obtained from FEM: σ_{fe}^*

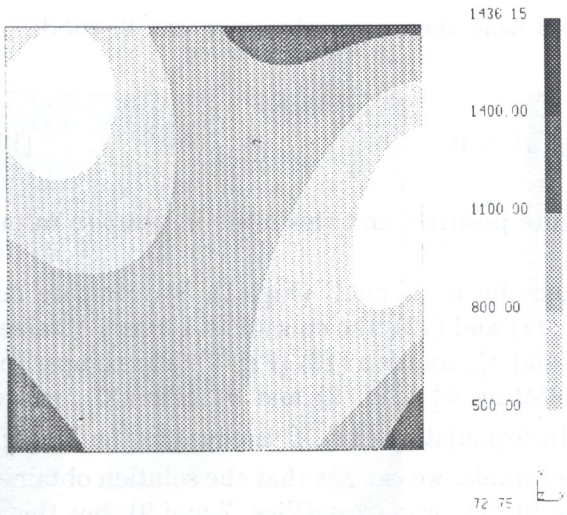

Fig. 3. Equivalent stress obtained from our simplified method: σ_{sm}^*

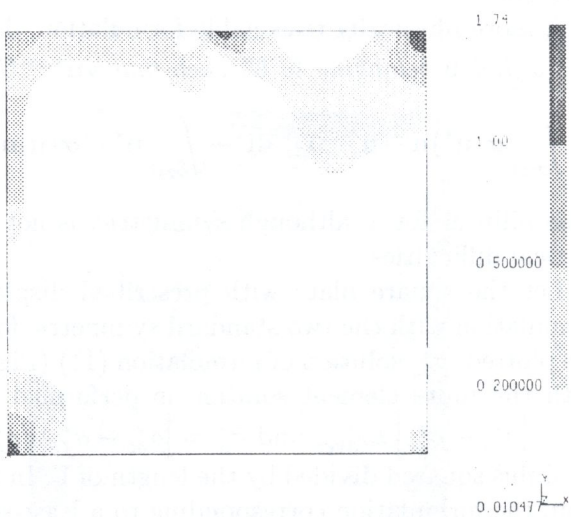

Fig. 4. Comparison between FEM and the simplified method: $\bar{\sigma}_1^*$

As a second example, the square plate is clamped at $y = 0$ and uniformly loaded along Γ by a shear stress (Fig. 5). In order to simplify the presentation, only the difference $\bar{\sigma}_1^*$ between finite element and our simplified method solution is plotted (Fig. 6). The results are correct inside the structure (the lightest zone corresponds to an error of less than 10 per cent). These two examples show that our method yielded an accurate computation of the interior effect.

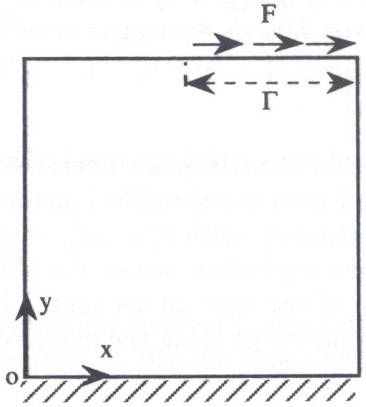

Fig. 5. Square with shear stress

4.2. Comparison with other formulations using Trefftz functions

In our approach, the approximation using Trefftz functions is representative of the interior effect. A variational formulation for a simple domain, which is consistent with this approximation and differs from the classical ones used in Trefftz methods [16,17], has been introduced.

There are several alternative variational formulations of the elastostatic problem used in Trefftz methods. Among these are two formulations used for one-domain structures, without substructuring or finite element discretization. These other standard symmetric formulations are compared with our formulation (3), by using the same set of Trefftz functions (9).

The first corresponds to a least-square fit and can be written as:

To find $\mathbf{u}$ *belonging to* U_e *such that* $\forall \mathbf{u}^* \in U_e$:

$$\beta^2 \int_{\partial_1 \Omega} \mathbf{u}^* \cdot (\mathbf{u} - \mathbf{u}_d)\, \mathrm{d}\Gamma + \int_{\partial_2 \Omega} \boldsymbol{\sigma}(\mathbf{u}^*)\mathbf{n} \cdot (\boldsymbol{\sigma}(\mathbf{u})\mathbf{n} - \mathbf{f}_d)\, \mathrm{d}\Gamma = 0\,, \tag{11}$$

where β is an arbitrary coefficient. For this symmetric formulation, a mechanical interpretation does not exist.

A more physically reasonable formulation, deduced from the potential energy, can be used:

To find $\mathbf{u}$ *belonging to* U_e *such that* $\forall \mathbf{u}^* \in U_e$:

$$\int_{\partial_1 \Omega} \boldsymbol{\sigma}(\mathbf{u}^*)\mathbf{n} \cdot (\mathbf{u} - \mathbf{u}_d)\, \mathrm{d}\Gamma - \int_{\partial_2 \Omega} \mathbf{u}^* \cdot (\boldsymbol{\sigma}(\mathbf{u})\mathbf{n} - \mathbf{f}_d)\, \mathrm{d}\Gamma = 0\,. \tag{12}$$

This bilinear form, although symmetric, is not definite positive, and this leads in practice to numerical difficulties.

Let the square plate with prescribed displacement be $\mathbf{u} \cdot x$ on Γ (Fig. 1). To compare our formulation with the two standard symmetric forms (11) and (12), the equivalent stresses obtained are plotted: σ_{1s}^* solution of formulation (11) (Fig. 7), and σ_{pe}^* solution (12) (Fig. 8). The comparison with the finite element solution is performed by plotting $\bar{\sigma}_2^*$ (Fig. 9) and $\bar{\sigma}_3^*$ (Fig. 10), where: $\bar{\sigma}_2^* = \left|\sigma_{1s}^* - \sigma_{fe}^*\right| / \sigma_{ave}^*$, and $\bar{\sigma}_3^* = \left|\sigma_{pe}^* - \sigma_{fe}^*\right| / \sigma_{ave}^*$. In formulation (11), β is equal to the Young's Modulus squared divided by the length of Γ. In this example, we can see that the solution obtained from the formulation corresponding to a least-square fit (11) is correct (Figs. 7 and 9), but this is not the case when using the formulation deduced from the potential energy (12) (Figs. 8 and 10). For the second example, where the square plate is clamped at $y = 0$ and uniformly loaded along Γ

by a shear stress (Fig. 5), we plot only $\bar{\sigma}_2^*$ in order to simplify the presentation. As opposed to the first example, the result $\bar{\sigma}_2^*$ obtained from the least-square fit is not correct (Fig. 11), while result $\bar{\sigma}_3^*$ obtained from the potential energy is correct.

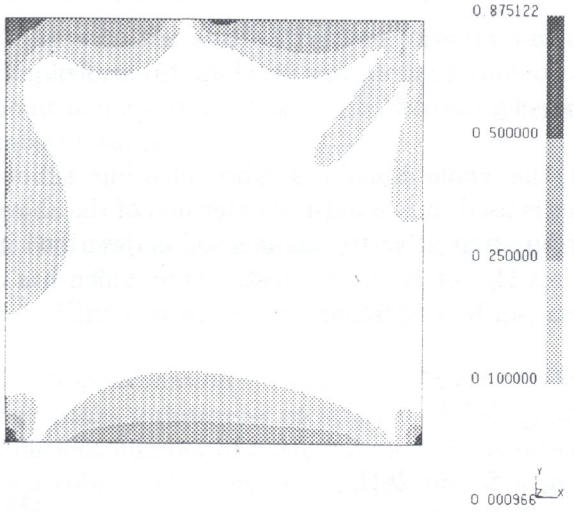

Fig. 6. Comparison between FEM and the simplified method: $\bar{\sigma}_1^*$

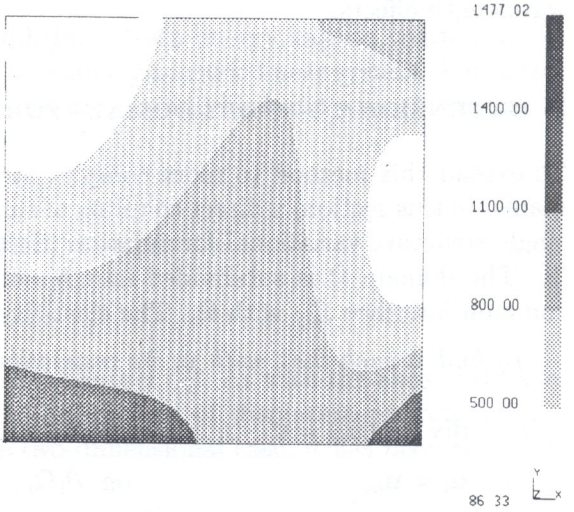

Fig. 7. Equivalent stress obtained from the least square fit: $\bar{\sigma}_{\text{ls}}^*$

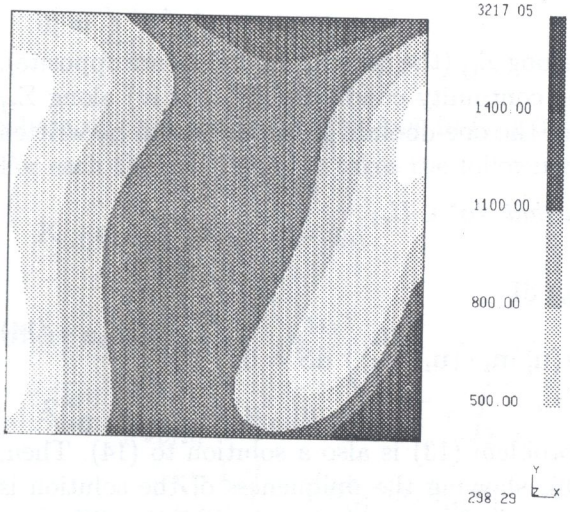

Fig. 8. Equivalent stress obtained from the potential energy: $\bar{\sigma}_{\text{pe}}^*$

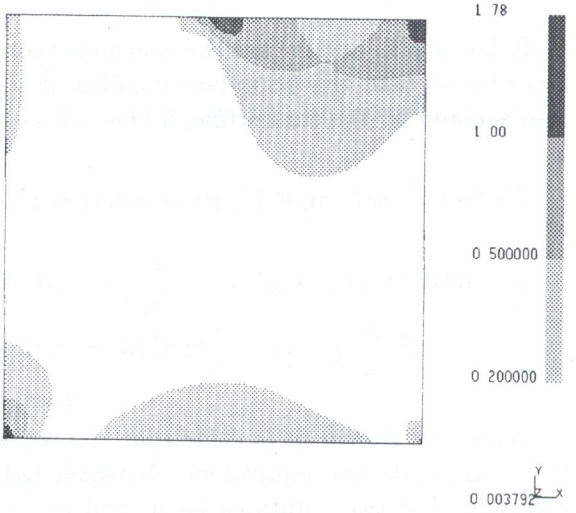

Fig. 9. Comparison between FEM and the least square fit: $\bar{\sigma}_2^*$

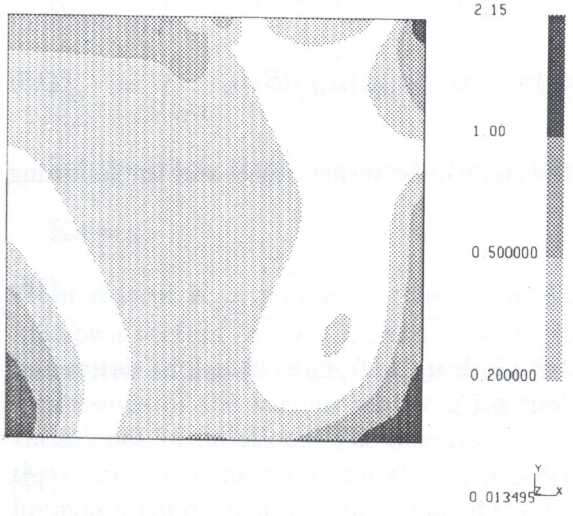

Fig. 10. Comparison between FEM and the potential energy: $\bar{\sigma}_3^*$

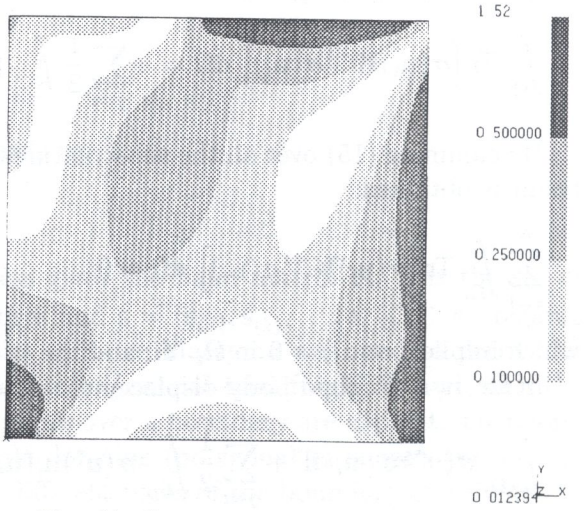

Fig. 11. Comparison between FEM and the least square fit

More generally, for all tested simple examples, our simplified method gives a correct result $\bar{\sigma}_1^*$ of less than or equal to 20 per cent inside the structure; this is not always the case for the two classical forms, (11) and (12). Our approximation enables a more accurate computation of the interior long wavelength effects.

5. Extension to multi-domain formulations

To extend this method to more complex structures, the whole domain is subdivided into subdomains. In this section, a direct coupling of subdomains is used. It is a natural extension of the above single-structure variational formulation (Section 3). An alternative to this method is described in [9]. The domain Ω is subdivided into N substructures Ω_i; let Ω_j be a substructure which has a common interface Σ_{ij} with Ω_i. The elasticity problem can be written as:

To find $\mathbf{u}$ *such that, with* $\mathbf{u}_i$ *its restriction in* Ω_i:

$$\begin{aligned}
&\text{i)} \quad \operatorname{div} \mathbf{K}\boldsymbol{\varepsilon}(\mathbf{u}_i) = 0 && \text{in } \Omega_i\,,\\
&\text{ii)} \quad \mathbf{u}_i = \mathbf{u}_{di} && \text{on } \partial_1\Omega_i\,, \quad \boldsymbol{\sigma}(\mathbf{u}_i)\,\mathbf{n}_i = \mathbf{f}_i \quad \text{on } \partial_2\Omega_i\,,\\
&\text{iii)} \quad \mathbf{u}_i = \mathbf{u}_j && \text{on } \Sigma_{ij}\,,\\
&\text{iv)} \quad \boldsymbol{\sigma}(\mathbf{u}_i)\,\mathbf{n}_i + \boldsymbol{\sigma}(\mathbf{u}_j)\,\mathbf{n}_j = 0 && \text{on } \Sigma_{ij}\,.
\end{aligned} \tag{13}$$

Relations iii) and iv) are the continuity conditions along Σ_{ij} (the normals $\mathbf{n}_i$ and $\mathbf{n}_j$ are opposite). In order to take the boundary conditions ii) and the continuity conditions iii) and iv) along Σ_{ij} into account at the same time, a generalised version of the one-domain formulation can be written as:

To find $\mathbf{u}$, *with* $\mathbf{u}_i \in U_e$ *its restriction in* Ω_i, *such that* $\forall \mathbf{u}^* \in U_e$,

$$\begin{aligned}
&\int_{\partial_1\Omega} \boldsymbol{\sigma}(\mathbf{u}^*)\mathbf{n}\cdot(\mathbf{u}_i - \mathbf{u}_{di})\,\mathrm{d}\Gamma + \int_{\partial_2\Omega} \mathbf{u}^*\cdot(\boldsymbol{\sigma}(\mathbf{u}_i^*)\mathbf{n}_i - \mathbf{f}_{di})\,\mathrm{d}\Gamma\\
&\qquad + \sum_{j\neq i}\frac{1}{2}\int_{\Sigma_{ij}} \Big\{\mathbf{u}^*\cdot\Big(\boldsymbol{\sigma}(\mathbf{u}_i^*)\mathbf{n}_i + \boldsymbol{\sigma}(\mathbf{u}_j^*)\mathbf{n}_j\Big) + \boldsymbol{\sigma}(\mathbf{u}_i^*)\mathbf{n}_i\cdot(\mathbf{u}_i - \mathbf{u}_j)\Big\}\,\mathrm{d}S = 0\,.
\end{aligned} \tag{14}$$

With this choice, it is clear that the solution to problem (13) is also a solution to (14). Then, to demonstrate the equivalence between (14) and (3), showing the uniqueness of the solution is sufficient. Let two solutions be $\mathbf{u}'$ and $\mathbf{u}''$, with $\mathbf{u}_i'$ and $\mathbf{u}_i''$ their restrictions in Ω_i , the difference $\mathbf{u}_i = \mathbf{u}_i' - \mathbf{u}_i''$ belongs to U_e and solves problem (14) with $\mathbf{u}_{di} = 0$, $\mathbf{f}_{di} = 0$. For $\mathbf{u}^* = \mathbf{u}_i$ and by using Stokes' formula, (14) gives:

$$\int_{\Omega_i} \operatorname{Tr}\left[\boldsymbol{\sigma}(\mathbf{u}_i)\mathbf{K}^{-1}\boldsymbol{\sigma}(\mathbf{u}_i)\right]\,\mathrm{d}\Omega = -\sum_{j\neq i}\frac{1}{2}\int_{\Sigma_{ij}} (\mathbf{u}_i\cdot\boldsymbol{\sigma}(\mathbf{u}_j)\mathbf{n}_j + \mathbf{u}_j\cdot\boldsymbol{\sigma}(\mathbf{u}_i)\mathbf{n}_i)\,\mathrm{d}S\,. \tag{15}$$

By summing (15) over all the substructures Ω_i, all the right-hand terms cancel and the following result is obtained:

$$\sum_{i=1}^{N}\int_{\Omega_i} \operatorname{Tr}\left[\boldsymbol{\sigma}(\mathbf{u}_i)\mathbf{K}^{-1}\boldsymbol{\sigma}(\mathbf{u}_i)\right]\,\mathrm{d}\Omega = 0 \tag{16}$$

which implies: $\boldsymbol{\sigma}(\mathbf{u}_i) = 0$ in Ω_i $\forall i$, and the problem (14) (with $\mathbf{u}_{di} = 0\,, \mathbf{f}_{di} = 0$) can be written as:
in $\Omega_i\,, \mathbf{u}_i \in S$ (rigid body displacement space) and $\forall \mathbf{u}^* \in U_e$:

$$\int_{\partial_1\Omega_i} \boldsymbol{\sigma}(\mathbf{u}^*)\mathbf{n}\cdot\mathbf{u}_i\,\mathrm{d}\Gamma + \sum_{j=i}\frac{1}{2}\int_{\Sigma_{ij}} \boldsymbol{\sigma}(\mathbf{u}^*)\mathbf{n}_i(\mathbf{u}_i - \mathbf{u}_j)\,\mathrm{d}S = 0\,. \tag{17}$$

The solution to (17) is:

$\mathbf{u}_i = 0$ in Ω_i, if the area of $\partial_1\Omega$ is different from zero,

$\mathbf{u}_i = \mathbf{u}_j$, if the area of $\partial_1\Omega$ is equal to zero.

As with the single-structure formulation, the equilibrium strain energy can be written in the simple form (6), and this variational formulation leads to a non-symmetric linear system. This latter point is not a drawback herein, because the structure has been subdivided into a small number of substructures.

6. Study of the solution for complex structures

6.1. Finite dimension study

The approximation consists of replacing, in (14), U_e by the subset U_e^p. As with the above problem, we obtain uniqueness of stresses. To demonstrate the uniqueness of displacement from (17), a sufficient number of basic functions is required. In the two-dimensional case, it has been shown [8] that subset U_e^3 is sufficient.

Let the polynomial expansion of the displacement $\mathbf{u}_i$ in each Ω_i be:

$$\mathbf{u}_i = \sum_{k=1}^{14} a_i^k \mathbf{u}_{(i)}^k ,$$

where $\mathbf{u}_{(i)}^k$ are the basic functions in Ω_i which belong to U_e^3 and a_i^k are the unknown coefficients. For each Ω_i, problem (14) takes the following form:

$$\mathbf{K}_{(ii)}\mathbf{a}_i + \sum_{j\neq i} \mathbf{K}_{(ij)}\mathbf{a}_j = \mathbf{s}_{(i)} , \tag{18}$$

where $\mathbf{a}_i = (a_i^1, a_i^2, \ldots, a_i^{14})^{\mathrm{T}}$ and:

$$\begin{aligned}
K_{(ii)}^{kl} &= \int_{\partial_1\Omega_i} \boldsymbol{\sigma}(\mathbf{u}_{(i)}^k)\mathbf{n}_i \cdot \mathbf{u}_{(i)}^l \,\mathrm{d}\Gamma + \int_{\partial_2\Omega_i} \mathbf{u}_{(i)}^k \cdot \boldsymbol{\sigma}(\mathbf{u}_{(i)}^l)\mathbf{n}_i \,\mathrm{d}\Gamma \\
&\quad + \sum_{j\neq i} \frac{1}{2} \int_{\Sigma_{(ij)}} \left\{ \mathbf{u}_{(i)}^k \cdot \boldsymbol{\sigma}(\mathbf{u}_{(i)}^l)\mathbf{n}_i + \boldsymbol{\sigma}(\mathbf{u}_{(i)}^k)\mathbf{n}_i \cdot \mathbf{u}_{(i)}^l \right\} \mathrm{d}S , \\
K_{ij}^{kl} &= \int_{\Sigma_{ij}} \left\{ \mathbf{u}_{(i)}^k \cdot \boldsymbol{\sigma}(\mathbf{u}_{(j)}^l)\mathbf{n}_j - \boldsymbol{\sigma}(\mathbf{u}_{(i)}^k)\mathbf{n}_i \cdot \mathbf{u}_{(j)}^l \right\} \mathrm{d}S , \\
s_{(i)}^k &= \int_{\partial_1\Omega_i} \boldsymbol{\sigma}(\mathbf{u}_{(i)}^k)\mathbf{n}_i \cdot \mathbf{u}_{di} \,\mathrm{d}\Gamma + \int_{\partial_2\Omega_i} \mathbf{u}_{(i)}^k \cdot \mathbf{f}_{di} \,\mathrm{d}\Gamma .
\end{aligned}$$

For the whole structure, the linear system (18) leads to:

$$\mathbf{K}\mathbf{a} = \mathbf{s} .$$

From matrix $\mathbf{K}_{(ii)}$ and $\mathbf{K}_{(ij)}$, the assembling process gives the band matrix $\mathbf{K}$, $\mathbf{a}$ is the set of unknown vectors $(\mathbf{a}_1, \mathbf{a}_2, \ldots, \mathbf{a}_N)^{\mathrm{T}}$ for N substructures and $\mathbf{s} = (\mathbf{s}_{(1)}, \mathbf{s}_{(2)}, \ldots, \mathbf{s}_{(N)})^{\mathrm{T}}$. As regards numerical implementation, the symbolic mathematics software Macsyma was used to derive the expressions of the various matrices associated with the polynomial trial functions and with the variational formulations. The integrals of the polynomials over a boundary are explicit. Therefore, there are few constraints on the shapes of the single domains (polygonal in shape) and on the boundary conditions (several types of conditions on different parts of the boundary of a domain).

6.2. Comparison with a finite element result

As an example, the structure shown in Fig. 12 is clamped on $y = 0$, and the displacement u_y (along y) on Γ is prescribed. The equivalent stress σ^*_{sm} obtained is compared with a finite element analysis σ^*_{fe}, and given in Fig. 13. In order to show the efficiency of the substructuring method, the structure is first a single element (without substructuring techniques). The obtained result $\bar{\sigma}^*_1 = |\sigma^*_{\text{sm}} - \sigma^*_{\text{fe}}/\sigma^*_{\text{ave}}$ is given in Fig. 14. It is clear that the difference between our solution and the finite element solution can be large inside the structure ($\bar{\sigma}^*_1$ greater than 25 per cent). To improve the solution, the same structure is divided into three substructures (dotted lines in Fig. 12); the resulting equivalent stress is given in Fig. 15 and $\bar{\sigma}^*_1$ in Fig. 16. A very good agreement is obtained inside the structure, but there are discontinuities through the interfaces between elements. The displacement and stress continuity conditions have not *a priori* been fulfilled at the interfaces, and discontinuities of solutions appear along the interfaces.

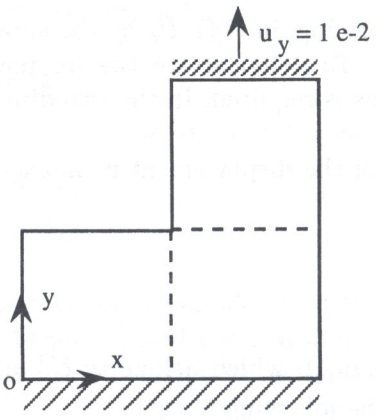

Fig. 12. Example using the substructuring method

6.3. Comparison with an exact solution

To study the behaviour of the simplified method, comparison with an exact solution is important. Let a given displacement vector $\bar{\mathbf{u}}$ be defined on the structure Ω. $\bar{\mathbf{u}}$ belongs to the finite dimension space U_e^N. Let $\bar{\mathbf{u}}_d$ on $\partial_1\Omega$ and $\bar{\mathbf{f}}_d$ on $\partial_2\Omega$ be the boundary conditions associated with the exact solution $\bar{\mathbf{u}}$.

Our problem then is:

To find $\mathbf{u}$, *with* $\mathbf{u}_i \in U_e^p$ *its restriction in* Ω_i, *such that*, $\forall \mathbf{u}^* \in U_e^p$,

$$\int_{\partial_1\Omega_i} \boldsymbol{\sigma}(\mathbf{u}^*)\mathbf{n}_i \cdot (\mathbf{u}_i - \bar{\mathbf{u}}_{di})\, \mathrm{d}\Gamma + \int_{\partial_2\Omega_i} \mathbf{u}^* \cdot (\boldsymbol{\sigma}(\mathbf{u}_i)\mathbf{n}_i - \mathbf{f}_{di})\, \mathrm{d}\Gamma + \sum_{j\neq i} \frac{1}{2} \int_{\Sigma_{ij}} \{\mathbf{u}^* (\boldsymbol{\sigma}(\mathbf{u}_i)\mathbf{n}_i + \boldsymbol{\sigma}(\mathbf{u}_j)\mathbf{n}_j) + \boldsymbol{\sigma}(\mathbf{u}_i^*)\mathbf{n}_i \cdot (\mathbf{u}_i - \mathbf{u}_j)\}\, \mathrm{d}S = 0\,. \tag{19}$$

The solution will be sought within the finite dimension space U_e^p. If $p \geq N$, then U_e^p includes the solution; it is the unique solution to problem (19). For $p < N$, $\bar{\mathbf{u}}$ cannot be the solution; in this case, the solution $\mathbf{u}_{\text{sol}}$ to (19) is compared to the exact solution $\bar{\mathbf{u}}$.

Let us consider a square plate. For plane stresses, we use the polynomial function with sets of degree lower than or equal to 3 which fulfill the governing differential equations U_e^3 (defined by (9)). Define a displacement solution $\bar{\mathbf{u}}$ belonging to U_e^4:

$$\bar{\mathbf{u}} = \frac{1}{2(1-\nu)^2} \begin{Bmatrix} (1-\nu^2)(x^4 - 3x^2y^2) \\ 4(1-\nu)xy^3 + (2(1+\nu)^2 - 8)x^3y \end{Bmatrix}. \tag{20}$$

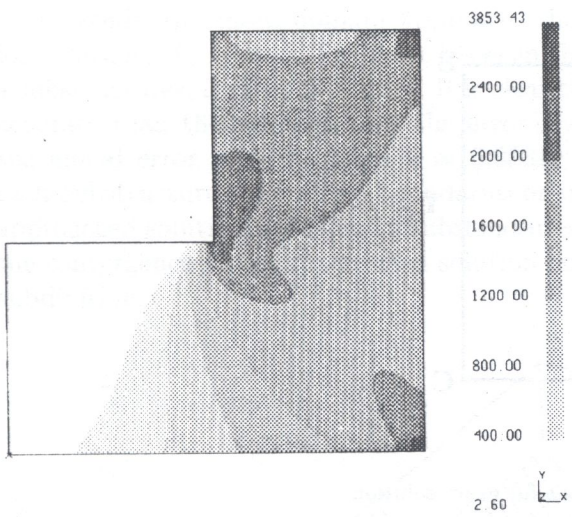

Fig. 13. Equivalent stress obtained from FEM: σ^*_{fe}

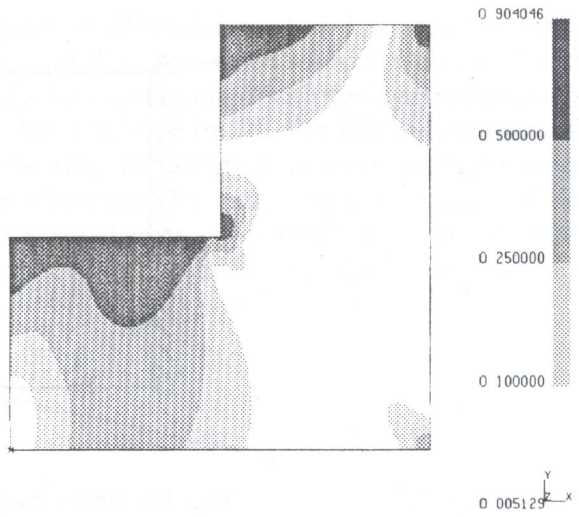

Fig. 14. Comparison to the simplified method, without substructuring: $\bar{\sigma}^*_1$

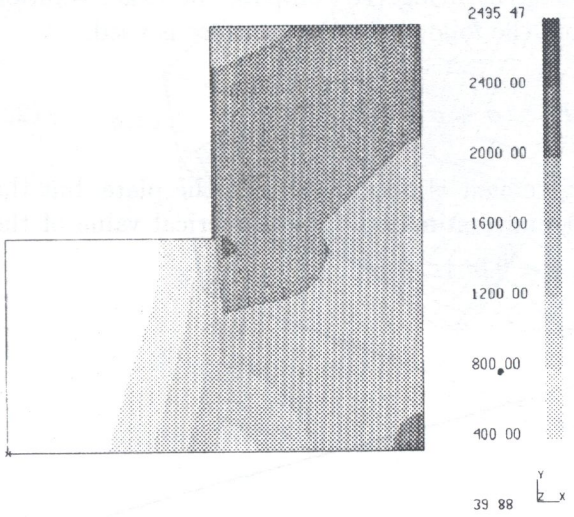

Fig. 15. Equivalent stress obtained from the substructuring method: σ^*_{sm}

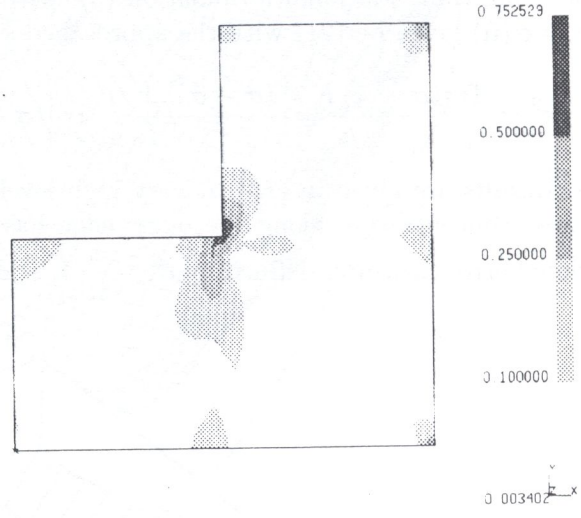

Fig. 16. Comparison to the simplified method, with substructuring: $\bar{\sigma}^*_1$

Obtained stresses are:

$$\boldsymbol{\sigma}(\bar{\mathbf{u}}) = \frac{E}{(1+\nu)} \begin{Bmatrix} (2+\nu)x^3 - 3xy^2 & -3(2+\nu)x^2y + y^3 \\ -3(2+\nu)x^2y + y^3 & -(3+2\nu)x^3 + 3(2+\nu)xy^2 \end{Bmatrix}. \tag{21}$$

From $\bar{\mathbf{u}}$ and $\boldsymbol{\sigma}(\bar{\mathbf{u}})$, boundary conditions are defined as:

on the side OA $(x = 0, 0 \leq y \leq 1)$: $\bar{\mathbf{u}}_d = 0$

on the side AB $(0 \leq x \leq 1, y = 1)$: $\bar{\mathbf{f}}_{d1} = \dfrac{E}{(1+\nu)} \begin{Bmatrix} -3(2+\nu)x^2 + 1 \\ -(3+2\nu)x^3 + 3(2+\nu)x \end{Bmatrix}$,

on the side BC $(x = 1, 0 \leq y \leq 1)$: $\bar{\mathbf{f}}_{d2} = \dfrac{E}{(1+\nu)} \begin{Bmatrix} (2+\nu) - 3y^2 \\ -3(2+\nu)y + y^3 \end{Bmatrix}$,

on the side CO $(0 \leq x \leq 1, y = 0)$: $\bar{\mathbf{f}}_{d3} = \dfrac{E}{(1+\nu)} \begin{Bmatrix} 0 \\ -(3+2\nu)x^3 \end{Bmatrix}$.

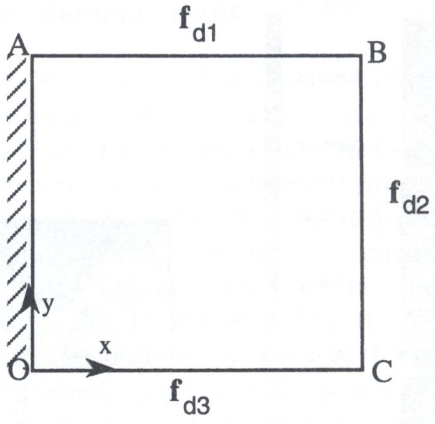

Fig. 17. Boundary conditions for exact solution

From these boundary conditions, the approached solution $\mathbf{u}_{\text{sol}}$ belonging to U_e^3 is calculated by using the variational formulation (3), without substructuring. To compare the exact solution $\bar{\boldsymbol{\sigma}} = \boldsymbol{\sigma}(\bar{\mathbf{u}})$ given by (21) with the approached solution, the following error measure is used:

$$\varepsilon^2 = \frac{\mathrm{Tr}\left[(\boldsymbol{\sigma} - \bar{\boldsymbol{\sigma}})\, K^{-1}\, (\boldsymbol{\sigma} - \bar{\boldsymbol{\sigma}})\right]}{\mathrm{Tr}\left[(\boldsymbol{\sigma} + \bar{\boldsymbol{\sigma}})\, K^{-1}\, (\boldsymbol{\sigma} + \bar{\boldsymbol{\sigma}})\right]} \frac{1}{\Omega} \int_\Omega \mathrm{Tr}\left[(\boldsymbol{\sigma} + \bar{\boldsymbol{\sigma}})\, K^{-1}\, (\boldsymbol{\sigma} + \bar{\boldsymbol{\sigma}})\right] \mathrm{d}\Omega\,. \tag{22}$$

Results are given in (18). A very high level of agreement is obtained inside the plate, but the stress concentration along the outer edge has been underestimated. The numerical value of the global error measure, defined by $e^2 = \dfrac{1}{\Omega} \displaystyle\int_\Omega \varepsilon^2 \, \mathrm{d}\Omega$, is $e = 0.064$.

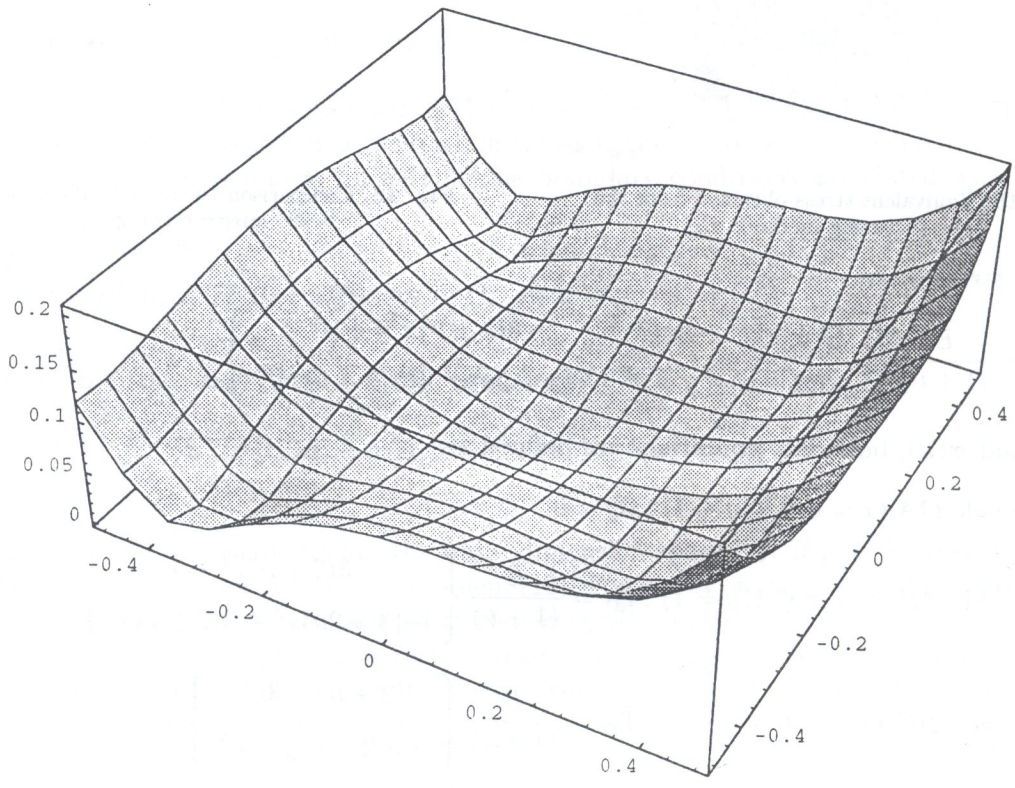

Fig. 18. Error measure, for a simple structure, between approached and exact solutions

To study the multi-domain approach, the structure is divided into 4 and 16 substructures; formulation (19) is used. The error between the exact and the approached solutions, obtained with 4 substructures, is given in Fig. 19. It is clear that the solution computed with this partition is more accurate than the previous one; the error level has been divided by 10. For this substructuring, the global error measure gives $e = 0.0081$. We note that the solution is more accurate inside each substructure than along boundaries or interfaces between elements. The computation of the approached solution, by using 16 substructures, gives a global error $e = 0.00097$. These results show the convergence of the approached solution on the exact solution; the error is divided by 8 at each subdivision.

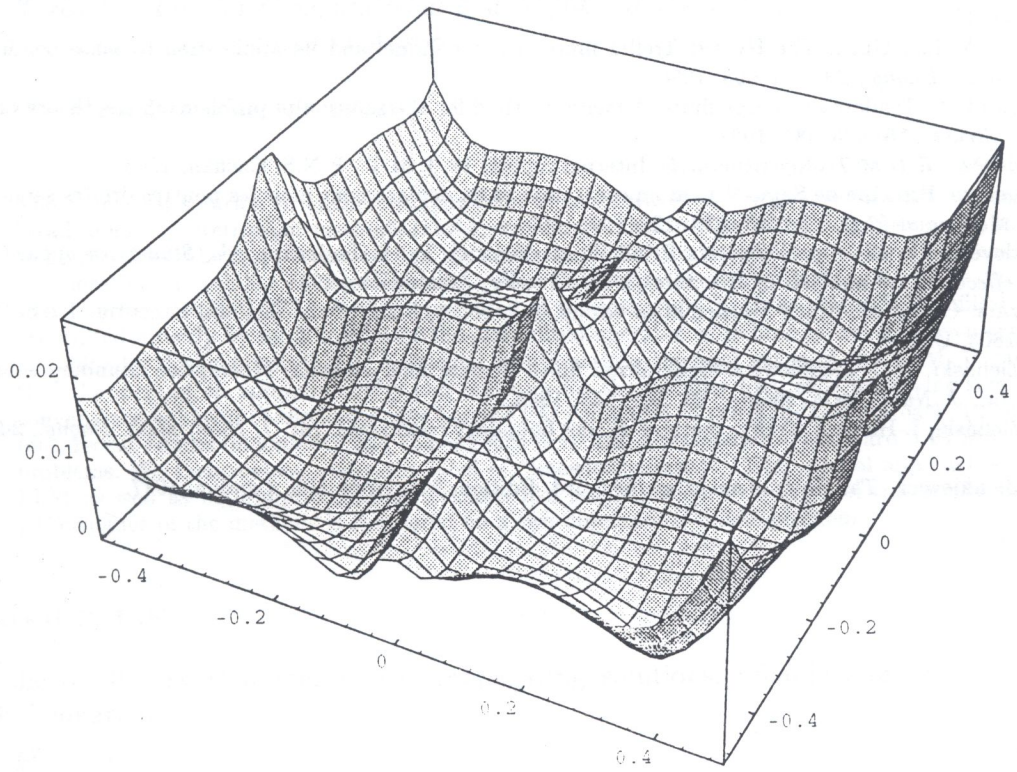

Fig. 19. Error measure, with 4 substructures, between approached and exact solutions

Conclusions

The simplified method presented herein allows a quick and correct approximation of the long wavelength effects in structures. It combines a Trefftz approximation with an original non-symmetric formulation. Comparison with other formulations proves the efficiency of the proposed approach. This study has been extended to plate structures for the computation of tools for sheet metal forming used in automotive industries. To determine small wavelength effects, which appear around the edges, another study [3] has been conducted through a post-processing approach using a technique initiated in [1].

References

[1] I. Babuska, A. Miller. The post-processing approach in the finite element method. Part 1: Calculation of displacements, stresses and other high derivatives of displacements. *Int. J. Num. Meth. Eng.*, **20**: 1085–1109, 1984.

[2] C.A. Brebbia, S. Walker, *Boundary element technique in Engineering.* Newne–Butterworth, London, 1980.

[3] G.E. Christian. *Sur une méthode de calcul des concentrations de contraintes.* Thèse de doctorat, Université Paris VI, Paris, 1993.

[4] G. Duvaut, J.L. Lions. *Les inéquations en mécanique et en physique.* Dunod, Paris, 1972.

[5] H. Gourgeon, I. Herrera. Boundary methods. C-complete systems for the biharmonic equation. In: C.A. Brebbia, ed., *Boundary Element methods*, 431–441. Springer–Verlag, 1981.

[6] I. Herrera, H. Gourgeon. Boundary methods. C-complete systems for Stokes problems. *Comp. Meth. Appl. Mech. Engng.*, **30**: 225–244, 1982.

[7] I. Herrera. Trefftz method. In: C.A. Brebbia, ed., *Topics in Boundary Element research*, vol. 1, chap. 10, 225–253. Springer–Verlag, 1984.

[8] C. Hochard, L. Proslier. A simplified analysis of plate structures using Trefftz functions. *Int. J. Num. Meth. Engng.*, **32**: 179–195, 1991.

[9] C. Hochard, P. Ladevèze, L. Proslier. A simplified analysis of elastic structures. *Eur. Journal Mech.*, **12**(4): 509–535, 1993.

[10] J. Jirousek, Lan Guex. The Hybrid–Trefftz finite element model and its application to plate bending. *Int. J. Num. Meth. Engng.*, **23**: 651–693, 1986.

[11] J. Jirousek, P. Teodorescu. Large finite elements method for the solution of problems in the theory of elasticity. *Comp. Struct.*, **15**: 575–587, 1982.

[12] P. Ladevèze. *R.D.M.Tridimensionnelle.* Internal report, 12, L.M.T., E.N.S. Cachan, 1983.

[13] P. Ladevèze. Principe de Saint-Venant en contrainte et en déplacement pour les poutres droites semi-infinies. *J. Appl. Mech. and Phys. (ZAMP)*, **33**: 132–139, 1985.

[14] P. Ladevèze. On the Saint-Venant's Principle in elasticity. In: P. Ladevèze, ed., *Studies in applied mech. 12: Local effects in the analysis of structures*,3–34. Elvesier, Amsterdam, 1985.

[15] Macsyma. Computer-Aided Mathematics Group. Symbolics, Inc., 8 New England Executive Park, Burlington, MA 01803, USA.

[16] A.P. Zieliński, O.C. Zienkiewicz. Generalized finite element analysis with T-complete boundary solution functions. *Int. J. Num. Meth. Engng.*, **21**: 509–528, 1985.

[17] A.P. Zieliński, I. Herrera. Trefftz method: fitting boundary conditions. *Int. J. Num. Meth. Engng.*, **24**: 871–891, 1987.

[18] O.C. Zienkiewicz, *The finite element method*, 3rd. Edition, Mc. Graw Hill, London, 1977.